

PAPER • OPEN ACCESS

## Surface radiative forcing of forest disturbances over northeastern China

To cite this article: Yuzhen Zhang and Shunlin Liang 2014 *Environ. Res. Lett.* **9** 024002

View the [article online](#) for updates and enhancements.

You may also like

- [Comparing the bulk radiated power efficiency in carbon and ITER-like-wall environments in JET](#)  
P Devynck, G Maddison, C Giroud et al.
- [Heat dissipation at a graphene–substrate interface](#)  
Zhiping Xu and Markus J Buehler
- [Nonlocal laser annealing to improve thermal contacts between multi-layer graphene and metals](#)  
Victor A Ermakov, Andrei V Alaferdov, Alfredo R Vaz et al.

# Surface radiative forcing of forest disturbances over northeastern China

Yuzhen Zhang<sup>1</sup> and Shunlin Liang<sup>1,2</sup>

<sup>1</sup> State Key Laboratory of Remote Sensing Science, College of Global Change and Earth System Science, Beijing Normal University, Beijing, China

<sup>2</sup> Department of Geographical Science, University of Maryland, College Park, USA

E-mail: [yuzhenzhang86@gmail.com](mailto:yuzhenzhang86@gmail.com)

Received 15 November 2013, revised 11 December 2013

Accepted for publication 6 January 2014

Published 17 February 2014

## Abstract

Forests provide important climate forcing through biogeochemical and biogeophysical processes. In this study, we investigated the climatic effects of forest disturbances due to changes in forest biomass and surface albedo in terms of radiative forcing over northeastern China. Four types of forest disturbances were considered: fires, insect damage, logging, and afforestation and reforestation. The mechanisms of the influence of forest disturbances on climate were different. ‘Instantaneous’ net radiative forcings caused by fires, insect damage, logging, and afforestation and reforestation were estimated at  $0.53 \pm 0.08 \text{ W m}^{-2}$ ,  $1.09 \pm 0.14 \text{ W m}^{-2}$ ,  $2.23 \pm 0.27 \text{ W m}^{-2}$ , and  $0.14 \pm 0.04 \text{ W m}^{-2}$ , respectively. Trajectories of CO<sub>2</sub>-driven radiative forcing, albedo-driven radiative forcing, and net forcing were different with time for each type of disturbance. Over a decade, the estimated net forcings were  $2.24 \pm 0.11 \text{ W m}^{-2}$ ,  $0.20 \pm 0.31 \text{ W m}^{-2}$ ,  $1.06 \pm 0.41 \text{ W m}^{-2}$ , and  $-0.47 \pm 0.07 \text{ W m}^{-2}$ , respectively. These estimated radiative forcings from satellite observations provided evidence for the mechanisms of the influences of forest disturbances on climate.

Keywords: forest disturbances, radiative forcing, surface albedo, forest biomass, northeastern China

## 1. Introduction

Forests influence climate through hydrological, biogeochemical, and ecosystem processes (Bonan 2008). These complex forest–atmosphere interactions can dampen or amplify climate change. Forests play an important role in mitigating climate change, because they can exert negative radiative forcing through carbon sequestration (Dixon *et al* 1993, Lal 2004, Streck and Scholz 2006). However, climatic impacts of forests are not limited to greenhouse gas reduction alone, and the overall climatic impacts of forests also depend on other effects, such as the warming effect due to lower albedo of forests and the evapotranspiration effect (Charney *et al* 1977, Schaeffer *et al* 2006, Thompson *et al* 2009).

Betts (2000) compared the carbon cycle and albedo effects of forestation in terms of radiative forcing and found that high-latitude forestation may intensify climate change instead of mitigating it, as intended. Bala *et al* (2007) simulated the climatic effects of global large-scale deforestation and found that warming effects of the carbon cycle are neutralized by the net cooling associated with changes in albedo and evapotranspiration. Gibbard *et al* (2005), Betts *et al* (2007) suggested that extratropical forestation could be less effective than expected or even counterproductive. If mitigating climate change is the sole objective, plantations should not be established in high-latitude regions (Jackson *et al* 2008, van Minnen *et al* 2008).

Climate change mitigation through forestry activities also carries the risk of carbon returning to the atmosphere because of disturbances to the forests (Canadell and Raupach 2008). Major forest disturbances, including forest fires, insect damage, disease outbreaks, droughts, and tropical storms,



Content from this work may be used under the terms of the [Creative Commons Attribution 3.0 licence](https://creativecommons.org/licenses/by/3.0/). Any further distribution of this work must maintain attribution to the author(s) and the title of the work, journal citation and DOI.

are expected to increase in frequency or intensity under changing climatic conditions (Dale *et al* 2001, Haughian *et al* 2012). Disturbance regimes range from succession after stand-replacing disturbances to gap dynamics related to the loss of individual trees (Angelstam and Kuuluvainen 2004). Such events make the situation complex. Little is known about the magnitude of these impacts on carbon stocks and surface albedo, and it is unclear whether these disturbances will generate either negative or positive radiative forcing.

Several studies have attempted to quantify the impacts of forest disturbances using observed data sets. Jin and Roy (2005) estimated an instantaneous regional surface radiative forcing of  $0.52 \text{ W m}^{-2}$  in northern Australia due to fire-induced albedo change. Randerson *et al* (2006) reported a negative radiative forcing of  $-5 \pm 2 \text{ W m}^{-2}$  due to changes in surface albedo during the first year after boreal forest fires, and provided evidence that spring and summer albedo remained elevated for approximately three decades after a fire. O'Halloran *et al* (2012) found a cooling effect (negative radiative forcing) after fires and beetle attacks in boreal forests with winter snow, and a local heating effect in a hurricane-damaged mangrove forest where both albedo and  $\text{CO}_2$  forcing were positive. In this study, we aim to quantify surface radiative forcing associated with both biomass change and albedo change to investigate the climatic impacts of four types of forest disturbances (forest fires, insect damage, logging, and afforestation and reforestation) over northeastern China.

## 2. Data and methods

### 2.1. Study area

Northeastern China consists of Heilongjiang, Jilin, and Liaoning provinces, as well as the eastern part of the Inner Mongolia Autonomous Region. It stretches about  $15^\circ$  from south to north and  $20^\circ$  from west to east (figure 1). The region is characterized by a continental monsoon climate, including warm temperate, temperate, and cold temperate zones from south to north and humid, semihumid, and semiarid zones from east to west. The annual mean temperature is  $5.2^\circ\text{C}$ , and the annual precipitation reaches 400–1000 mm, 80% of which falls between May and September (Chen *et al* 2011). This region is completely dominated by seasonal snow cover, and snow cover disappears in the summer (Che *et al* 2008).

The forests in the region are cold-temperate conifer mixed forests, temperate conifer and broadleaf mixed forests, and warm-temperate deciduous broadleaf mixed forests. Forests of these types account for about 30% of forest land in China. Northeastern China is important to the nation as a key source for timber, a broad habitat and a potential carbon sequestration region.

### 2.2. Mapping forest disturbances

Many algorithms have been proposed to detect forest disturbances from remote sensing data (Mildrexler *et al* 2009, Hansen *et al* 2010, Verbesselt *et al* 2010, Masek *et al* 2011). In this study, we considered four types of forest disturbances,

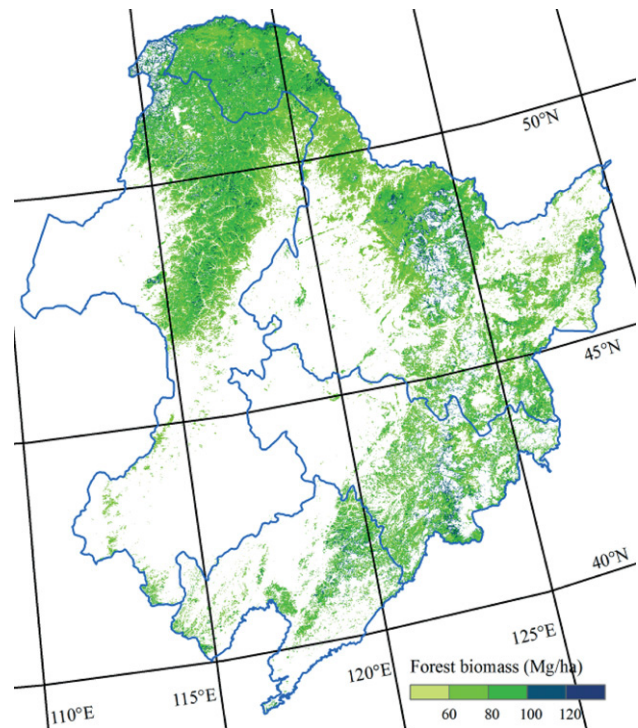


**Figure 1.** Study area. The background information is the mean value of forest biomass between 2001 and 2010.

including forest fires, insect damage, forest logging, and afforestation and reforestation, which were detected from Moderate Resolution Imaging Spectroradiometer (MODIS) data. The MODIS global disturbance index (MGDI) algorithm was used to detect the locations of forest disturbances. It was based on annual maximum MODIS Land Surface Temperature (LST) data and annual maximum MODIS Enhanced Vegetation Index (EVI) data (Mildrexler *et al* 2007, 2009). The underlying principle was that LST decreased with an increase in vegetation density through latent heat transfer. MGDI values from 2001 to 2010 were calculated using maximum composite LSTs and EVIs from 2000 to 2010.

Because different kinds of forest disturbances influence forest ecosystems in different ways, we need to distinguish them. MODIS fire products were used to separate fire disturbances and non-fire disturbances. Both the MODIS active fire product and the MODIS burned area product were used. The former detected active fires and other thermal anomalies, and the latter gave the extent of burn scars over a specified time period (Justice *et al* 2002). Fire pixels, which were categorized as high confidence or nominal confidence in the active fire product and labeled as burned in the MODIS burned area product, were used to locate fire disturbances in this study. Non-fire disturbances were separated using MODIS Vegetation Continuous Field (VCF) data (Hansen *et al* 2003). VCF data contain a percentage of vegetation types for each pixel. Compared to traditional discrete classification data, this data set is more appropriate for describing changes in forest cover. In contrast to large-scale logging, insect infestations represent a type of non-instantaneous disturbance event that does not cause an immediate reduction in forest cover (Mildrexler *et al* 2009). Based on these properties, pixels with a large decrease

**Table 1.** Summary of disturbance information and associated radiative forcing for logging, afforestation and reforestation, fire, and insect damage.

Disturbance type	Logging	Afforestation and reforestation	Fire	Insect damage
Annual area disturbed (million hectare)	0.15	2.89	1.26	0.57
Instantaneous albedo-driven radiative forcing ( $W m^{-2}$ )	$-0.22 \pm 0.19$	$0.62 \pm 0.03$	$-0.92 \pm 0.06$	$0.65 \pm 0.12$
Instantaneous CO <sub>2</sub> -driven radiative forcing ( $W m^{-2}$ )	$2.45 \pm 0.08$	$-0.48 \pm 0.01$	$1.44 \pm 0.02$	$0.43 \pm 0.03$
Decadal albedo-driven radiative forcing ( $W m^{-2}$ )	$-1.48 \pm 0.33$	$0.56 \pm 0.04$	$-0.52 \pm 0.08$	$-0.56 \pm 0.28$
Decadal CO <sub>2</sub> -driven radiative forcing ( $W m^{-2}$ )	$2.53 \pm 0.08$	$-1.03 \pm 0.03$	$2.76 \pm 0.08$	$0.76 \pm 0.03$

in forest cover were used to identify where deforestation or large-scale logging occurred, and pixels with MGDI values larger than a certain threshold were used to identify areas affected by insects and diseases. We used both absolute and relative changes in VCF to quantify the loss of forest cover.

The key to separating disturbances caused by insects and diseases from those caused by large-scale logging was to determine the threshold value for the MGDI data and the threshold value for changes in MODIS VCF data, respectively. The kappa coefficient was a good way to quantify the level of agreement, and thus used to determine the thresholds in this study (Congalton 1991, Kennedy *et al* 2007). Kappa coefficients were highest when threshold for the MGDI and for changes in VCF were  $-15$  and  $-85\%$ . So these thresholds were used to detect large-scale logging and insect damage. Unlike logging and insect damage, afforestation and reforestation can contribute to an increase in forest cover. After masking out those pixels of recovery from other disturbances, pixels with a sharp increase in forest cover were considered to be afforestation and reforestation regions.

### 2.3. Calculation of surface radiative forcing

Radiative forcing is often used to assess the climatic impacts of disturbances per-unit area and compare the anthropogenic and natural drivers of climate change (Forster *et al* 2007). Here, we use surface forcing to quantify the instantaneous perturbation of the surface radiative balance by a forcing agent. For each type of forest disturbance, two types of surface radiative forcing were considered: CO<sub>2</sub>-driven radiative forcing related to the loss of forest biomass carbon to the atmosphere, and albedo-driven radiative forcing related to changes in land cover properties. Net forcing was defined as the sum of albedo-driven radiative forcing and CO<sub>2</sub>-driven radiative forcing.

Pixel-by-pixel albedo and biomass values before disturbance were extracted as reference values. Changes in albedo and biomass caused by forest disturbances were evaluated by comparing albedo and biomass values before disturbance (reference value) and after disturbance.

**2.3.1. Albedo-driven radiative forcing.** Global LAnd Surface Satellite (GLASS) albedo data were chosen to characterize surface albedo (Liang *et al* 2013). It covers the years 1981–2010 at horizontal resolutions between 1 km and 5 km and 8-day (spatial and temporal) resolutions. Preliminary validation results indicate high accuracy and robustness of the data set (Liu *et al* 2013). We used GLASS albedo data from 2000–2010 at 1-km resolution. The 8-day GLASS albedo values were averaged to produce monthly mean values. Surface radiative forcing (RF) from changes in monthly albedo was calculated using

$$RF = R_s \times (\alpha_1 - \alpha_2), \tag{1}$$

where  $R_s$  is surface incoming solar radiation,  $\alpha_1$  is monthly surface albedo before disturbances, and  $\alpha_2$  is monthly surface albedo after disturbances. Global Energy and Water Exchanges (GEWEX) Surface Radiation Budget (SRB) Release-3.0 data sets provided monthly mean surface incoming solar radiation at  $1^\circ$  by  $1^\circ$  grid cells from July 1983 to December 2007. We calculated GEWEX-SRB multiyear monthly means from 1983 onward to derive climatology of incoming solar radiation. After the calculation of monthly radiative forcing on the basis of monthly albedo and monthly incoming solar radiation, seasonal changes in radiative forcing were average values of the corresponding months.

**2.3.2. CO<sub>2</sub>-driven radiative forcing.** In this study, we mapped forest biomass during 2000–2010 (figure 1) using the random forests (RF) model. The model was developed with field data, geoscience laser altimeter system (GLAS) data, and MODIS surface reflectance data. Further details can be found in one of our previous publications (Zhang *et al* 2013). Changes in forest biomass caused by forest disturbance can lead to the absorption or emission of CO<sub>2</sub>. CO<sub>2</sub>-driven radiative forcing due to changes in forest biomass was calculated as follows (Myhre *et al* 1998):

$$RF = 5.35 \ln(1 + \Delta C / C_0), \tag{2}$$

$$\Delta C = M_a \times \Delta CO_2 / (M_C \times m_a), \tag{3}$$



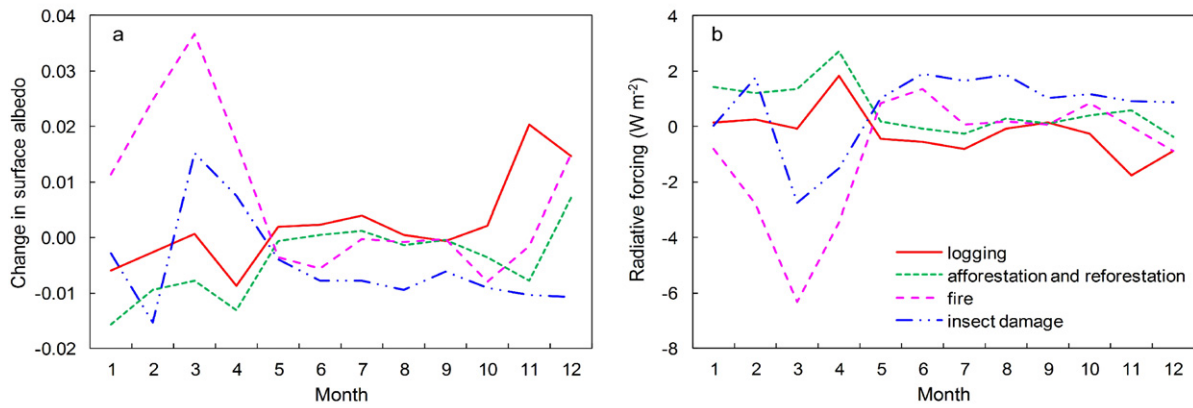


**Figure 2.** Instantaneous monthly albedo change and associated radiative forcing at the surface.

where  $\Delta C$  is the atmospheric enrichment in  $\text{CO}_2$  after tree combustion,  $C_0$  is the reference  $\text{CO}_2$  concentration,  $M_a$  is the molecular mass of dry air,  $M_c$  is the molecular mass of carbon,  $m_a$  is the mass of the atmosphere, and  $\Delta\text{CO}_2$  is the change in  $\text{CO}_2$  (in grams) resulting from biomass change.

**2.3.3. Uncertainty analysis.** Products derived from MODIS were the main data source used to detect and distinguish forest disturbances, so some minor changes cannot be reflected at the coarse scale. Besides, the threshold we chose might cause some uncertainty, although we adopted some methods to reduce the uncertainty. To evaluate the uncertainty of changes in albedo and biomass, as well as the associated radiative forcing, caused by the uncertainty of forest disturbances, we used the bootstrapping method (Efron and Tibshirani 1986). Uncertainties of estimates are standard deviations of bootstrap samples.

### 3. Results and discussions

During the period 2000–2010, about 1.26 million ha of forests were disturbed by fires, according to the MODIS fire product (table 1). They accounted for 1.92% of the forests of northeastern China. Fire disturbance resulted in a decrease in forest biomass ( $14.12 \pm 0.24 \text{ Mg ha}^{-1}$ ) and a resultant positive radiative forcing ( $1.44 \pm 0.02 \text{ W m}^{-2}$ ). Insects damaged 0.87% of forests in this region, and 0.24% of forests underwent large-scale logging. Insects and logging caused decreases in forest biomass of  $6.01 \pm 0.27 \text{ Mg ha}^{-1}$  and  $26.85 \pm 0.86 \text{ Mg ha}^{-1}$ , and associated radiative forcings of  $0.43 \pm 0.03 \text{ W m}^{-2}$  and  $2.45 \pm 0.08 \text{ W m}^{-2}$ , respectively (table 1). On the other hand, afforestation and reforestation caused a biomass increase of  $1.71 \pm 0.05 \text{ Mg ha}^{-1}$  and a negative forcing of  $0.48 \pm 0.01 \text{ W m}^{-2}$  (table 1). Among the four types of forest disturbances, the impact of logging was the largest in terms of  $\text{CO}_2$ -driven radiative forcing, followed by fires, insect damage, and afforestation and reforestation.

Changes in surface albedo due to forest disturbances and the associated radiative forcing were different in each month (figure 2). Forest disturbances had a minor effect on

summer albedo. The changes were steady and relatively small for each type of forest disturbance. However, the effects on winter albedo and early spring albedo were large, probably because of snow cover (figures 2 and 3). Albedo increased in March after insect damage and increased in December after logging. Albedo in both March and December increased after fire disturbances (figure 2). Autumn albedo decreased after fires, insect damage, and afforestation and reforestation, but increased after logging disturbances (figure 2).

Changes in albedo fluctuations were observed along the time since disturbances (figure 3). During the first decade after forest disturbances, autumn albedo increased for forest logging. For insect damaged forests, autumn albedo increased after five years since disturbance. Whereas for fire disturbance, autumn albedo decreased after several years because of forest recovery. In afforestation and reforestation regions, changes in autumn albedo were mostly below zero. We calculated a significant positive trend of change in summer albedo after logging and insect damage. The trend of change in summer albedo caused by afforestation and reforestation increased. The trend of summer albedo increased for seven years following fire disturbance but then decreased. Changes in spring albedo were just above zero for logging, insect damage, and fire disturbance, but below zero in afforestation and reforestation regions, except at some turning points. Because of the large influence of forest disturbances on spring albedo and winter albedo, changes in annual albedo tended to respond similarly with them, but with a smaller magnitude (figure 3).

Changes in annual surface albedo and the associated radiative forcing were compared with  $\text{CO}_2$ -driven radiative forcing (figure 4). Results showed that the radiative forcings from albedo change and  $\text{CO}_2$  release had the same order of magnitude, and  $\text{CO}_2$ -driven radiative forcing was relatively stable for each type of disturbance, whereas albedo-driven radiative forcing fluctuated widely. Therefore, overall trends of net forcing mostly followed those of albedo-driven radiative forcing. For the case of fire, biomass decreased after fire, and radiative forcing due to biomass change was positive. This development could result in warming of the regional climate. Albedo was elevated in all seasons except autumn, and this difference was further enhanced with time. This

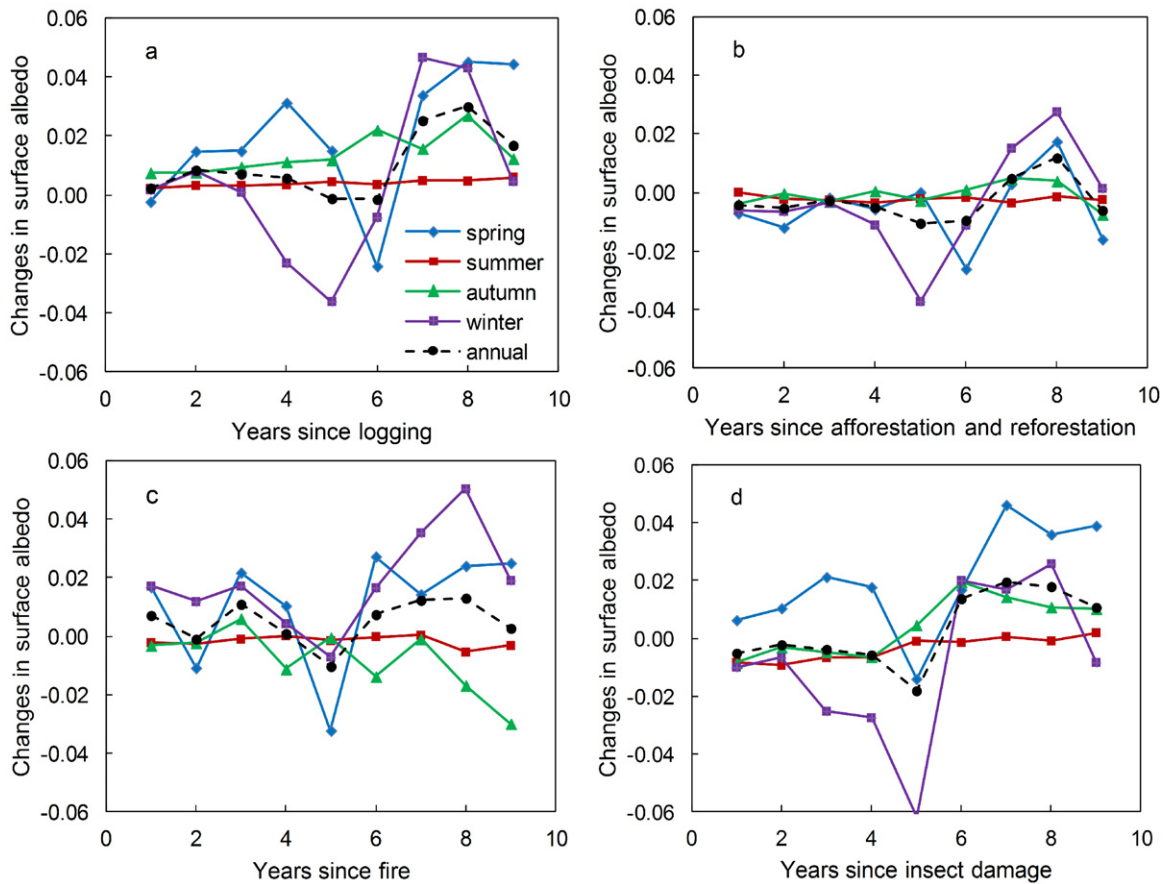


**Figure 3.** Changes in albedo during forest recovery since forest disturbances. (a) Logging, (b) afforestation and reforestation, (c) fire, and (d) insect damage.

outcome resulted in an annual negative radiative forcing of  $-0.92 \pm 0.06 \text{ W m}^{-2}$  (table 1). Combined changes in annual albedo and forest biomass contributed to an instantaneous net warming effect ( $0.53 \pm 0.08 \text{ W m}^{-2}$ ), and this warming effect continued because of the lasting loss of biomass in the following years. More  $\text{CO}_2$  was absorbed and stored as biomass by afforestation and reforestation, which caused a negative  $\text{CO}_2$ -driven radiative forcing. The net forcing fluctuated around zero during the first six years after tree planting. However, we observed a sharp decrease in net radiative forcing, and thus a net cooling effect, in the seven years after tree planting. For insect damage, the net forcing was positive during the first five years after disturbance and negative after the first five years. For forest logging, the associated radiative forcing revealed a warming climate effect caused by the decrease in forest biomass.

Compared with albedo-driven forcing,  $\text{CO}_2$ -driven forcing was relatively stable, because changes in forest biomass were not evident as changes in surface albedo (figure 4). Turning points of changes in albedo in spring and winter (figure 3) and the associated radiative forcing (figure 4) were observed around 5–6 years after disturbances. The mechanisms were complicated. Several reasons might account for the phenomenon. Snow cover was an important factor. This is because if forest biomass or forest cover did not change, but

snow cover changed annually, then albedo in spring or winter would increase substantially. The variation in snow cover can explain the results of forest logging in figures 3 and 4. But for afforestation and reforestation, mechanisms were different. The turning point partly suggested the relative role of changes in the introduction, previous studies indicated the albedo effect overwhelmed biomass effect in boreal and temperate forests. But as time goes by the biomass effect seems to dominate instead of albedo effect (figures 3 and 4). If this is the case, then we should not doubt the warming climate effects of large-scale afforestation in high latitude regions. However, we only focused on the northeastern China, and did not investigate the situation in other regions. Moreover, a decade was not long enough for us to make such a firm conclusion.

#### 4. Conclusions

In this study, we estimated the climatic effects of forest disturbances, including fires, insect damage, logging, and afforestation and reforestation, caused by changes in forest biomass and surface albedo in terms of radiative forcing. Results indicated that radiative forcings resulting from change in albedo and  $\text{CO}_2$  release were of the same order of magnitude. The ‘instantaneous’ net forcings of albedo-driven radia-

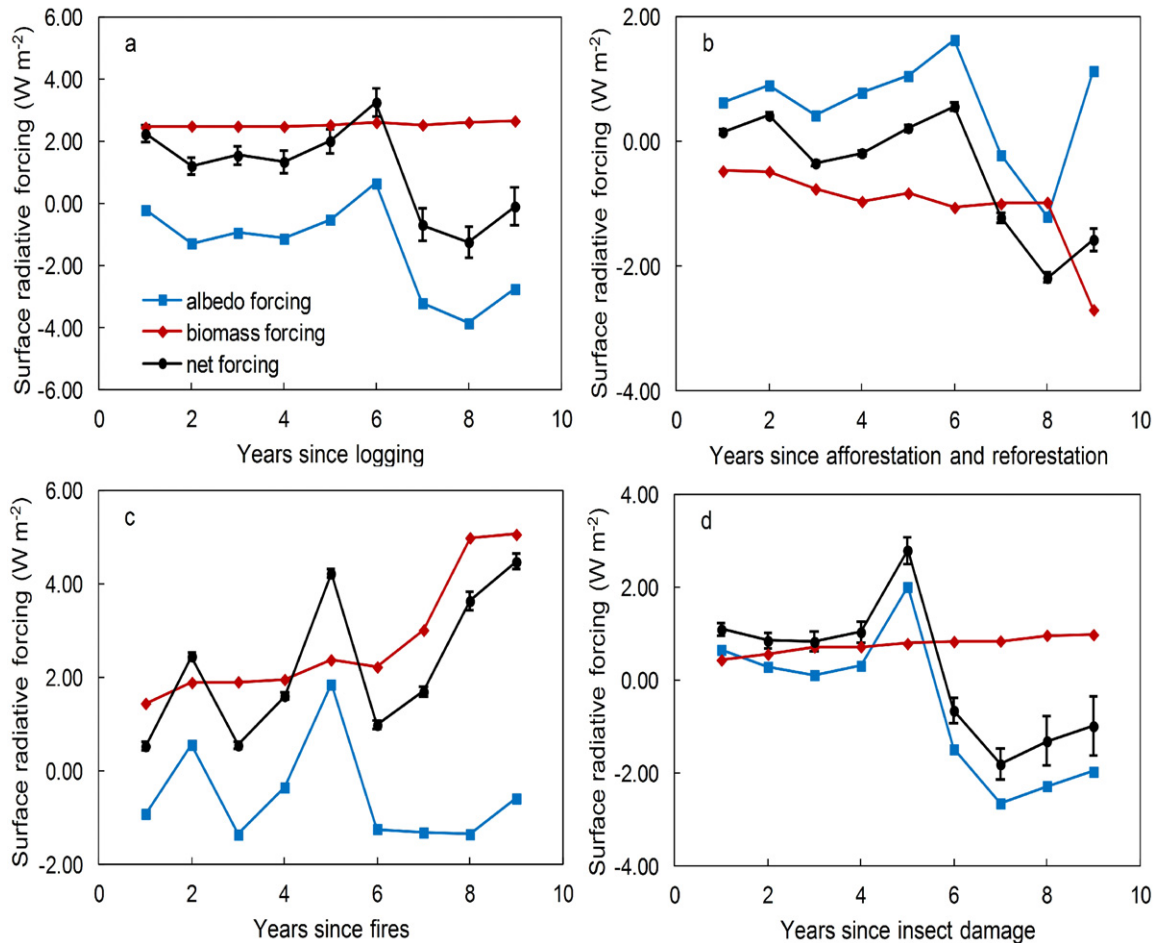


**Figure 4.** Radiative forcing associated with albedo change and biomass change caused by logging (a), afforestation and reforestation (b), fires (c) and insect damage (d).

tive forcing and CO<sub>2</sub>-driven radiative forcing were  $0.53 \pm 0.08 \text{ W m}^{-2}$ ,  $1.09 \pm 0.14 \text{ W m}^{-2}$ ,  $2.23 \pm 0.27 \text{ W m}^{-2}$ , and  $0.14 \pm 0.04 \text{ W m}^{-2}$  for fires, insect damage, logging, and afforestation and reforestation, respectively. During the first four or five years after disturbances, net forcings were positive for fires, insect damage, and logging, but negative for afforestation and reforestation. Trajectories of net forcings were different with time for these disturbances. Mechanisms were also different for each type of disturbance.

The forcings we estimated in this study were pixel based. When extended to a regional forcing or global forcing, the ratio of disturbed area to the area of this region or the surface area of the Earth should be multiplied.

We only considered the climatic effects due to changes in forest biomass and surface albedo in this study. We assumed that loss of forest biomass affected the atmosphere instantaneously. However, the situation is far more complicated than this case. This finding should be further investigated in future studies. Also, some possible forcing agents, such as aerosols and evapotranspiration, were neglected. More agents and more complicated scenarios must be included in further studies.

**Acknowledgments**

We are very grateful for anonymous reviewers for their constructive comments and suggestions. This study is funded by the National High Technology Research and Development Program 2013AA122800.

**References**

Angelstam P and Kuuluvainen T 2004 Boreal forest disturbance regimes, successional dynamics and landscape structures: a European perspective *Ecol. Bull.* **51** 117–36  
 Bala G, Caldeira K, Wickett M, Phillips T J, Lobell D B, Delire C and Mirin A 2007 Combined climate and carbon-cycle effects of large-scale deforestation *Proc. Natl Acad. Sci.* **104** 6550–5  
 Betts R A 2000 Offset of the potential carbon sink from boreal forestation by decreases in surface albedo *Nature* **408** 187–90  
 Betts R A, Falloon P D, Goldewijk K K and Ramankutty N 2007 Biogeophysical effects of land use on climate: model simulations of radiative forcing and large-scale temperature change *Agricult. Forest Meteorol.* **142** 216–33  
 Bonan G B 2008 Forests and climate change: forcings, feedbacks, and the climate benefits of forests *Science* **320** 1444–9

- Canadell J G and Raupach M R 2008 Managing forests for climate change mitigation *Science* **320** 1456–7
- Charney J, Quirk W J, Chow S h and Kornfield J 1977 A comparative study of the effects of albedo change on drought in semi-arid regions *J. Atmos. Sci.* **34** 1366–85
- Che T, Xin L, Jin R, Armstrong R and Zhang T 2008 Snow depth derived from passive microwave remote-sensing data in China *Ann. Glaciol.* **49** 145–54
- Chen C, Lei C, Deng A, Qian C, Hoogmoed W and Zhang W 2011 Will higher minimum temperatures increase corn production in Northeast China? An analysis of historical data over 1965–2008 *Agricult. Forest Meteorol.* **151** 1580–8
- Congalton R G 1991 A review of assessing the accuracy of classifications of remotely sensed data *Remote Sensing Environ.* **37** 35–46
- Dale V H, Joyce L A, McNulty S, Neilson R P, Ayres M P, Flannigan M D, Hanson P J, Irland L C, Lugo A E and Peterson C J 2001 Climate change and forest disturbances *BioScience* **51** 723–34
- Dixon R K, Andrasko K J, Sussman F G, Lavinson M A, Trexler M C and Vinson T S 1993 Forest sector carbon offset projects: near-term opportunities to mitigate greenhouse gas emissions *Water Air Soil Pollut.* **70** 561–77
- Efron B and Tibshirani R 1986 Bootstrap methods for standard errors, confidence intervals, and other measures of statistical accuracy *Stat. Sci.* **1** 54–75
- Forster P *et al* 2007 Changes in atmospheric constituents and in radiative forcing *Climate Change 2007: The Physical Science Basis* ed S D Solomon, D Qin, M Manning, Z Chen, M Marquis, K B Averyt, M Tignor and H L Miller (Cambridge: Cambridge University Press)
- Gibbard S, Caldeira K, Bala G, Phillips T J and Wickett M 2005 Climate effects of global land cover change *Geophys. Res. Lett.* **32** L23705
- Hansen M C, DeFries R S, Townshend J R G, Carroll M, Dimiceli C and Sohlberg R A 2003 Global percent tree cover at a spatial resolution of 500 meters: first results of the MODIS vegetation continuous fields algorithm *Earth Interact.* **7** 1–15
- Hansen M C, Stehman S V and Potapov P V 2010 Quantification of global gross forest cover loss *Proc. Natl Acad. Sci.* **107** 8650–5
- Haughian S R, Burton P J, Taylor S W and Curry C 2012 Expected effects of climate change on forest disturbance regimes in British Columbia *J. Ecosystems Manage.* **13** 1–24
- Jackson R B *et al* 2008 Protecting climate with forests *Environ. Res. Lett.* **3** 044006
- Jin Y and Roy D P 2005 Fire-induced albedo change and its radiative forcing at the surface in northern Australia *Geophys. Res. Lett.* **32** L13401
- Justice C O, Giglio L, Korontzi S, Owens J, Morisette J T, Roy D, Descloitres J, Alleaume S, Petitcolin F and Kaufman Y 2002 The MODIS fire products *Remote Sens. Environ.* **83** 244–62
- Kennedy R E, Cohen W B and Schroeder T A 2007 Trajectory-based change detection for automated characterization of forest disturbance dynamics *Remote Sens. Environ.* **110** 370–86
- Lal R 2004 Soil carbon sequestration to mitigate climate change *Geoderma* **123** 1–22
- Liang S *et al* 2013 A long-term Global Land Surface Satellite (GLASS) data-set for environmental studies *Int. J. Digit. Earth* **6** (supl.) 5–33
- Liu Q, Wang L, Qu Y, Liu N, Liu S, Tang H and Liang S 2013 Preliminary evaluation of the long-term GLASS albedo product *Int. J. Digit. Earth* **6** (supl.) 69–95
- Masek J G *et al* 2011 Recent rates of forest harvest and conversion in North America *J. Geophys. Res.: Biogeosci.* **116** G00K03
- Mildrexler D J, Zhao M, Heinsch F A and Running S W 2007 A new satellite-based methodology for continental-scale disturbance detection *Ecol. Appl.* **17** 235–50
- Mildrexler D J, Zhao M and Running S W 2009 Testing a MODIS global disturbance index across North America *Remote Sens. Environ.* **113** 2103–17
- Myhre G, Highwood E J, Shine K P and Stordal F 1998 New estimates of radiative forcing due to well mixed greenhouse gases *Geophys. Res. Lett.* **25** 2715–8
- O'Halloran T L *et al* 2012 Radiative forcing of natural forest disturbances *Glob. Change Biol.* **18** 555–65
- Randerson J T *et al* 2006 The impact of boreal forest fire on climate warming *Science* **314** 1130–2
- Schaeffer M, Eickhout B, Hoogwijk M, Strengers B, van Vuuren D, Leemans R and Opsteegh T 2006 CO<sub>2</sub> and albedo climate impacts of extratropical carbon and biomass plantations *Glob. Biogeochem. Cycles* **20** GB2020
- Streck C and Scholz S M 2006 The role of forests in global climate change: whence we come and where we go *Int. Affairs* **82** 861–79
- Thompson M P, Adams D and Sessions J 2009 Radiative forcing and the optimal rotation age *Ecol. Econom.* **68** 2713–20
- van Minnen J, Strengers B, Eickhout B, Swart R and Leemans R 2008 Quantifying the effectiveness of climate change mitigation through forest plantations and carbon sequestration with an integrated land-use model *Carbon Balance Manage.* **3** 3
- Verbesselt J, Hyndman R, Newnham G and Culvenor D 2010 Detecting trend and seasonal changes in satellite image time series *Remote Sens. Environ.* **114** 106–15
- Zhang Y *et al* 2014 Forest biomass mapping of northeastern China using GLAS and MODIS data *IEEE J. Sel. Top. Appl. Earth Obs. Remote Sens.* **7** 140–52